

## Molecular docking of SARS-CoV-2 proteins against selected ligands

<sup>1</sup>M. Ibtisam Khan, <sup>1</sup>N. Rajesh, <sup>2</sup>Anu Prasanna Vankara and <sup>1\*</sup>K. Riazunnisa

<sup>1\*</sup>Department of Biotechnology and Bioinformatics,

<sup>2\*</sup>Department of Zoology, Yogi Vemana University, Vemanapuram,  
YSR district -516005 (India)

\*Corresponding author: E-mail [khateefriaz@gmail.com](mailto:khateefriaz@gmail.com);  
[krbtbi@yogivemanauniversity.ac.in](mailto:krbtbi@yogivemanauniversity.ac.in)  
Contact: 09966863416

### Abstract

The outburst of COVID-19 (SARS-CoV-2) creates an unrivalled cause to human health all across the world and society. The growth of proper treatments is criticized in condition. Available drugs were present but with severe adverse effects. Hence in order to reduce an alternative medication is needed. Spike protein, Nucleocapsid protein, RNA-dependent-RNA-polymerase (RdRp), Mpro (Main protease), PLpro (Papain-like protease) are the proteins coronavirus (COVID-19) has various functions in its life cycle. Spike protein is an envelope protein that mostly interacts with the assembly of the virus and plays a crucial role in propounding the host cells and starting off with infection. RdRp is involved in genome expression like RNA synthesis, capping and proofreading. Mpro mediates the replication of virus and transcription. PLpro plays an important role in processing polyproteins of virus, maturation and virus assemblage. Hence in order to reduce the side effects, the present study focused on the molecular docking of selected ligands with coronavirus proteins. Autodock vina was used for docking proteins and ligands of COVID-19. Among various ligands, carbamic acid shows the least binding affinities *i.e.*, -10.7 kcal/mol with spike protein. The docking results indicate that the active binding pockets presuppose the amino acid residues – Asn142, Asp2, Thr24, Thr25, Thr26, Thr45, Asn37, Arg80, Trp29, Thr84, Arg188, Thr190, Arg262, Arg259, Arg88, Arg107, Arg319, Ile292, Glu323, Thr332, Ile357, Ala4, Ala40, Thr49, Thr57, Ile94, Ile130 and Glu118. Eventually, for the initial time, this computational study assumes the perspective of carbamic acid as a therapeutic strategy that acts against SARS-CoV-2. Network interactions

of spike protein reveal that transmembrane proteases were involved in protein-protein interaction with spike protein of SARS-CoV-2. Further optimization of these protein-protein interactions and docking could lead to promising drugs against SARS-CoV-2.

**Key words :** COVID-19, spike protein, RdRp, Mpro, PLpro, Autodock vina, binding affinity, carbamic acid.

COVID-19, an encapsulated single-stranded positive RNA sense virus belonging to the coronaviridae family, is currently the focus of significant global attention<sup>2</sup>. The WHO (World Health Organization) announced the outburst of the pandemic because of the increasing number of cases and its effects like spreading, high chances of transmission, all around the globe and insufficient vaccines or medications for the treatment of the disease. COVID-19 is phylogenetically related to the family of Nidovirales and comes under Betacoronaviruses<sup>8</sup>. COVID-19 has different varieties of structural and functional proteins *i.e.*, spike protein (S), envelope protein (E), membrane protein (M) and nucleocapsid protein (N)<sup>12</sup>. The genome size is 40KB which ciphers for dissimilar structural and accessory proteins. COVID-19 enters the cells of humans by attaching to a specific surface spike protein to an ACE2 receptor and host cell membrane fusion. The spike protein is known as a transmembrane protein with two end terminals – N-exo and C-endo terminals. The first end terminal with the S1 subunit contains RBD whereas the second end terminal with the S2 subunit encourages the fusion of membrane. The S1 subunit binding of spike protein to human cell receptors results in virus-human cell fusion. However, following virus endocytosis, the S2 subunit, whatever is esteemed by heptad repeats regions that assemble like a hair-pin

helical structure which is a six-helix bundle that assists the function of membrane within the host cell<sup>2</sup>. Later, it was identified that the COVID-19 with receptor binding domain and spike protein is high or low is same as that of SARS-CoV, in spite of differences with amino acids at some important residues. Moreover, forge ahead in docking methods' accuracy, reliability, and precision over the past few years which had made it a viable option for designing structural drugs<sup>9</sup>.

#### *Protein retrieval :*

The protein sequences (Spike protein, Nucleocapsid protein, RdRp, Mpro, PLpro) of coronavirus was retrieved from UniprotKB which is a freely available and accessed public database which is hand-operated and explicated. It can be obtained directly from (<http://uniprot.org/>)<sup>4</sup>. The protein sequence was obtained in FASTA format which is additionally used for docking swotting.

#### *Physico-chemical characterization :*

Computational investigation for physico-chemical properties of spike protein, RdRp, Mpro and PLpro was carried out using the server ExPASy. It has many online tools that assume few specific properties like Isoelectric point (pI), molecular weight (M.Wt),

peptide mass, amino acid composition, extinction coefficient, atomic composition, instability index, grand average hydropathy, the total number of positive and negative residues, and so on. ProtParam tool is used for the protein sequence in physico-chemical properties using FASTA format<sup>6</sup>.

#### *Determination of active sites analysis :*

CASTp (Computer Atlas of Surface Topography of proteins) server<sup>14</sup> was used for 3D structure of proteins, mostly the protein binding sites which were explored and deployed on its structural consortium of template and model construct. It was used to allow and discover the binding sites, structural surface pockets, active sites, area, shape and volume of every pocket and armpit of proteins. It can also be used to compute the number, mouth openings boundary of every pocket, reachable molecular surface and area. The specific perception of the docking furnishes the active site analysis.

#### *Docking :*

In order of priority, to get exact outputs, all the experiments of docking were executed with the reverted properties. The docking time for one ligand and protein was approximately 15-20 minutes. Autodock vina on a Linux center with an Intel Core R processor (1.30 GHz) and 8 GB RAM whereas FlexX was run on Windows 11 accoutred with an Intel® Core™ processor (1.30 GHz) and 7.68 GB of RAM<sup>5,15</sup>.

The mediator process, such as pdbqt files for protein preparation, ligands preparation

and grid box formation were completed using a graphical user interface (GUI) program in AutoDock Tools (ADT). AutoDock Tools allot the polar hydrogens, integrated Kollman charges, solvation parameters and fragmental volumes to the protein. The program saved the prepared file in PDBQT format. Using grid box for the construction of the grid map we used AutoGrid. The grid size is to be set at 60x60x60 for xyz points with the grid spacing set at 0.375 Å and the grid center was nominated at the xyz dimensions and the values were -1.095, -1.554 and 3.894. A grid scoring was pre-mediated from the structure of the ligand to keep down the time of computation. Autodock vina was used for docking protein and ligand data along with the parameters of grid box in the configuration (config) file. Autodock Vina working with repeated local investigation global optimizer. Throughout the docking approach, proteins and ligands both were rigid in structure. The least binding energy or binding affinity was pulled out and lined up with the structure of receptor for the additional survey.

#### *Network interactions :*

STRING (<https://string-db.org/>) is a biological database that is used to build the protein-protein interactions network for non-identical and identified assumed protein interactions<sup>13</sup>. RING (<https://ring.biocomputingup.it/submit>) is used to inspect the residue-residue interaction of spike protein, RdRp, Mpro and PLpro and was generated with a network called Cyto Scape v3.1.0<sup>3</sup>.

Physico-chemical parameters were pre-planned using Prot Param analysis, a tool of the ExpASy server and the information is

illustrated in Table-1. Isoelectric point (pI) was calculated which is an important parameter at which the proteins are stable and compact, means with least solubility and zero mobility in an electrofocusing system. Isoelectric point is the pH at which the charge on the protein is zero, no matter that the protein is covered with charge. The assessed pI value of spike protein (6.24), Mpro (6.04), PL pro (5.33) were acidic in nature, and nucleocapsid (10.07) was basic in nature. This information will be very beneficial for the development of a buffer system for the refinement of protein by the isoelectric focussing method.

The stability of proteins in the test tube was estimated on the basis of the instability index (II) of protein<sup>16</sup>. In this method, the occurrence of certain dipeptides is unstable which was compared to the stable ones, and provides the weight value of instability. By using weight value, it becomes possible to estimate the instability index. Protein with an instability index value of less than 40 is said to be stable and those with more than 40 are supposed to be unstable. The instability index value ranges from 11.36 to 41.55 for the antioxidant protein of *Pisum sativum*. This analysis concluded that Catalase (P25890 and COSTY9) are unstable proteins, and all the other proteins studied are stable. The protein instability index value for spike protein, RdRp, Mpro, Plpro is less than 40 hence stable proteins whereas nucleocapsid protein instability index value is greater than 40 hence unstable proteins.

The aliphatic index (AI) suggests the thermostability of a protein<sup>16</sup>. It is well-defined as the relative volume of a protein occupied by aliphatic side chains (alanine, leucine, isoleucine and valine). The value of the

aliphatic index for the antioxidant proteins of *Pisum sativum* varies from the range of 52.53 to 97.26. All the proteins showed a very high aliphatic index which means they are stable at a very wide range of temperatures. The least GRAVY (Grand Average of Hydropathy) index value recommends that it is much better protein interactions with the water molecules. The GRAVY index value is more in nucleocapsid protein and Plpro such that they interact with water molecules followed by Mpro, RdRp and spike protein (Table-1).

Auto Dock vina was identified as the outstanding performance for carrying out the blind docking, it generated poses and confine the deepest good at 5 Å of the binding pocket and it almost generated 50-70% perfect docking poses. The two-dimensional (2D) view of protein-ligand interactions of the perfect poses formed by all four studied procedures is illustrated in Fig 1. As openly delineated in the figure, all the molecules showed the same binding mode. Moreover, important interactions can be available between the atoms and the residues which personally engage in the mechanism of the catalytic enzyme. The ligand-enzyme complex is preserved mainly by hydrogen bonds and hydrophobic interactions.

The docking results are presented in terms of binding energies and the amino acid residues present at the predicted active site of the protein. Among all the proteins, carbamic acid showed the least binding energy (-10.7 kcal/mol) to the predicted active site of the protein (Table 2-6). It has formed five hydrogen bonds with Thr49, Thr57, Ile94, Ile130 and Glu118 amino acid residues which are available at the predicted active site of the protein<sup>10</sup>. Nucleoca-psid protein showed the least binding energy (-9.8 kcal/mol) with

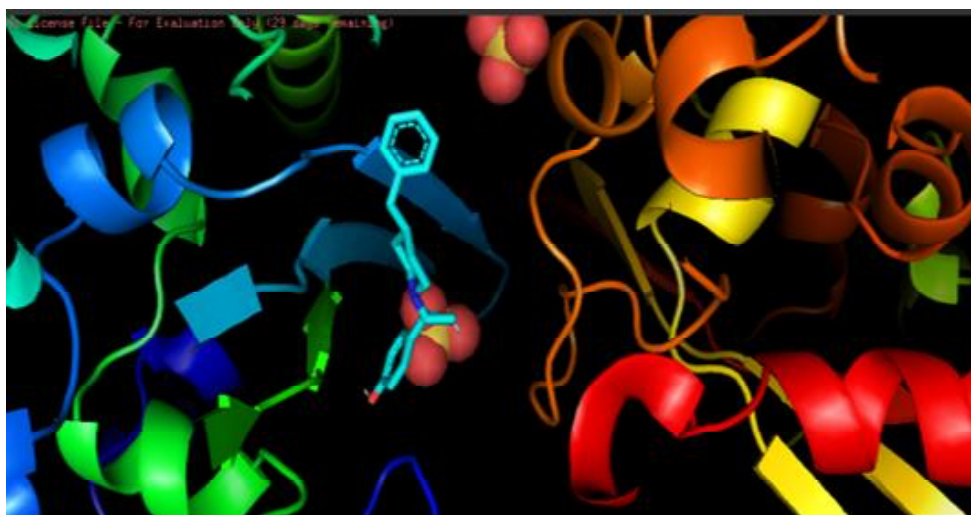


Fig. 1. Molecular docking of carbamic acid with spike protein of covid-19

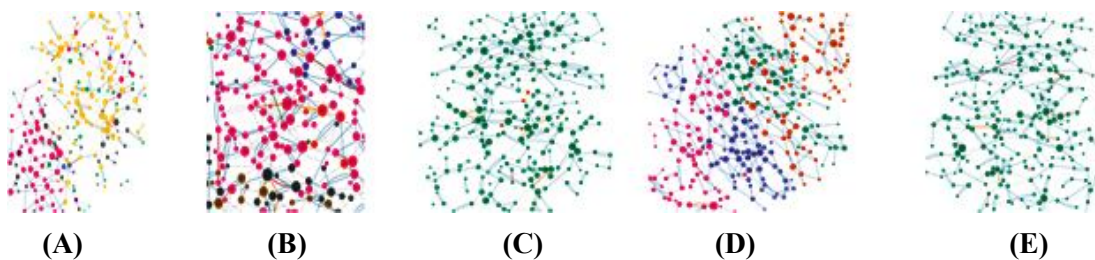


Fig. 2. Protein –protein network interactions of covid-19 proteins by using Cytoscape Spike protein (B) Nucleocapsid protein (C) RdRp protein (D) Mpro (E)PL pro.

carbamic acid<sup>7</sup> forming four hydrogen bonds (Ile292, Glu323, Thr332 and Ile357) (Table 3). RdRp showed the least binding energy with ONO-5334 (-8.9 kcal/mol)<sup>1</sup>. The ONO-5334 showed two hydrogen bonds (Trp29, Thr84). The docking results are in terms of binding energy and the amino acid interaction residues which are present at the protein assumed active site. ONO-5334 showed the least binding affinity (-7.3 kcal/mol)<sup>1</sup> to the assumed active site of the protein. It has formed 5 hydrogen bonds with Thr24, Thr25, Thr26,

Thr45 and Thr190 amino acid residues which are present at the assumed active site of the protein. The docking results of PLpro protein are in terms of binding energy and the amino acid residues interacting with the assumed active site of the protein. Avitinib showed the least binding affinity (-8.4 kcal/mol)<sup>11</sup> to the assumed active site of the protein. It has formed four hydrogen bonds with Thr25, Thr26, Thr45 and Thr24 amino acid residues which are present at the assumed active site of the protein.

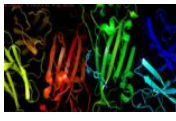
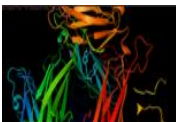
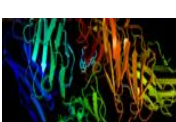
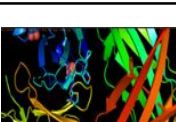
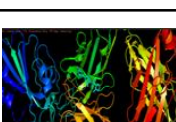



Table-1. Physicochemical Characterisation of Covid-19 proteins

Physico-chemical properties	Spike protein	Nucleo-capsid protein	RdRp	Mpro	PLpro
Number of amino acid residues	1273	419	7093	4405	4439
Molecular weight	141178.47	45625.70	-	489988.91	499208.23
Theoretical PI	6.24	10.07	-	6.04	5.33
Total number of positively charged residues	105	36	391	450	364
Total number of negatively charged residues	110	60	338	407	460
Formula	C <sub>6636</sub> H <sub>9770</sub> N <sub>1656</sub> O <sub>1894</sub> S <sub>54</sub>	C <sub>1971</sub> H <sub>3137</sub> N <sub>607</sub> O <sub>629</sub> S <sub>7</sub>	-	C <sub>21982</sub> H <sub>34326</sub> N <sub>5654</sub> O <sub>6524</sub> S <sub>243</sub>	C <sub>22728</sub> H <sub>34820</sub> N <sub>5622</sub> O <sub>6491</sub> S <sub>266</sub>
Total number of atoms	19710	6351	-	68729	69927
Instability index	33.10	55.09	33.74	34.92	30.84
Aliphatic index	84.67	52.53	86.81	88.99	97.26
Grand average of Hydropathy (GRAVY)	-0.079183	-0.971	-0.021	-0.023	0.213

From the spike protein of COVID-19, it was identified that 21 nodes and 77 edges through the STRING database. The different scale of color green to yellow to red denotes the number of connections for each node which probably ranges from 1 to 56. For spike protein, 6889 genes for the druggable genome are present. For kinases and associates, 792 genes are present. Transmembrane protease serine 2 plays an important role in the protein sample and the spike protein is selected as an input. It has been found that around 5 matches approx.

of TMPRSS has been extracted from the UniProt server. From the nucleocapsid protein of COVID-19, it is identified that 11 nodes and 14 edges, RdRp, it is identified that 11 nodes and 28 edges dicer like proteins (DCL) plays an important role in protein and found approx. 2 matches of DCL which has been extracted from UniProt server. RdRp also added the network interaction as their main chief for it. From the Mpro, it is identified that 4 nodes and 4 edges, for PLpro 11 nodes and 18 edges were identified.

Table-2. Molecular docking of selected ligands with Spike protein  
PDB ID: 7M3I and their binding energies

Ligand	Protein-Ligand Interactions	Interacting amino acids	Binding energies (kcal/mol)
Galidesivir		Lig - Cys136, Asp152, Pro175, Val206, Ser185, Val161, Val160, Leu134, Lys131, Ser211 Rec - Pro9, Asp216, Phe377, Ser11, Thr203, Trp187, Val129, Leu127, Ser196, Gln200, Asn205	-7.8
Ifenprodil		Lig - Cys136, Asp152, Pro175, Val206, Ser185, Val161, Val160, Leu134, Lys131, Ser211 Rec - Pro9, Asp216, Phe377, Ser11, Thr203, Trp187, Val129, Leu127, Ser196, Gln200, Asn205	-7.5
Avitinib		Lig - Cys136, Asp152, Pro175, Val206, Ser185, Val161, Val160, Leu134, Lys131, Ser211 Rec - Pro9, Asp216, Phe377, Ser11, Thr203, Trp187, Val129, Leu127, Ser196, Gln200, Asn205	-7.1
ONO-5334		Lig - Cys136, Asp152, Pro175, Val206, Ser185, Val161, Val160, Leu134, Lys131, Ser211 Rec - Pro9, Asp216, Phe377, Ser11, Thr203, Trp187, Val129, Leu127, Ser196, Gln200, Asn205	-8.0
Thalidomide		Lig - Cys136, Asp152, Pro175, Val206, Ser185, Val161, Val160, Leu134, Lys131, Ser211 Rec - Pro9, Asp216, Phe377, Ser11, Thr203, Trp187, Val129, Leu127, Ser196, Gln200, Asn205	-7.9
Vidofludimus		Lig - Cys136, Asp152, Pro175, Val206, Ser185, Val161, Val160, Leu134, Lys131, Ser211 Rec - Pro9, Asp216, Phe377, Ser11, Thr203, Trp187, Val129, Leu127, Ser196, Gln200, Asn205	-7.9
Apremilast		Lig - Cys136, Asp152, Pro175, Val206, Ser185, Val161, Val160, Leu134, Lys131, Ser211 Rec - Pro9, Asp216, Phe377, Ser11, Thr203, Trp187, Val129, Leu127, Ser196, Gln200, Asn205	-8.0
Ibuprofen		Lig - Cys136, Asp152, Pro175, Val206, Ser185, Val161, Val160, Leu134, Lys131, Ser211 Rec - Pro9, Asp216, Phe377, Ser11, Thr203, Trp187, Val129, Leu127, Ser196, Gln200, Asn205	-8.2

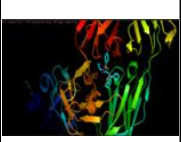
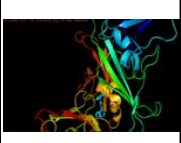

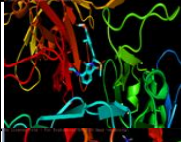

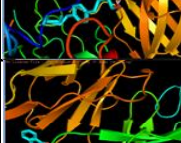
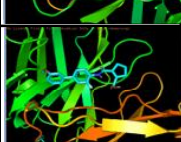


Ruxolitinib		Lig - Cys136, Asp152, Pro175, Val206, Ser185, Val161, Val160, Leu134, Lys131, Ser211 Rec - Pro9, Asp216, Phe377, Ser11, Thr203, Trp187, Val129, Leu127, Ser196, Gln200, Asn205	-8.3
Brensocaticib		Lig - Cys136, Asp152, Pro175, Val206, Ser185, Val161, Val160, Leu134, Lys131, Ser211 Rec - Pro9, Asp216, Phe377, Ser11, Thr203, Trp187, Val129, Leu127, Ser196, Gln200, Asn205	-8.4
Carbamic acid		Lig - Cys136, Asp152, Pro175, Val206, Ser185, Val161, Val160, Leu134, Lys131, Ser211 Rec - Pro9, Asp216, Phe377, Ser11, Thr203, Trp187, Val129, Leu127, Ser196, Gln200, Asn205	-10.7

Table-3. Molecular docking of selected ligands with Nucleocapsid protein PDB ID: 6WZ9 and their binding energies

Ligand	Protein-ligand interactions	Interacting amino acids	Binding energies (kcal/mol)
Ifenprodil		Rec – Ala251, Arg262, Ile292, Glu323, Pro364; Lig – Arg259, Pro279, Arg319, Gly321, Trp330, Thr332, Ile357, Lys361, Pro279, Met317, Gly335, Phe346, Val350, Tyr360, Gln306, Met317, Thr334, Asp340, Gln349	-7.5
Avitinib		Rec – Ala251, Arg262, Ile292, Glu323, Pro364; Lig – Arg259, Pro279, Arg319, Gly321, Trp330, Thr332, Ile357, Lys361, Pro279, Met317, Gly335, Phe346, Val350, Tyr360, Gln306, Met317, Thr334, Asp340, Gln349	-7.5
ONO-5334		Rec – Ala251, Arg262, Ile292, Glu323, Pro364; Lig – Arg259, Pro279, Arg319, Gly321, Trp330, Thr332, Ile357, Lys361, Pro279, Met317, Gly335, Phe346, Val350, Tyr360, Gln306, Met317, Thr334, Asp340, Gln349	-7.9
Thalidomide		Rec – Ala251, Arg262, Ile292, Glu323, Pro364; Lig – Arg259, Pro279, Arg319, Gly321, Trp330, Thr332, Ile357, Lys361, Pro279, Met317, Gly335, Phe346, Val350, Tyr360, Gln306, Met317, Thr334, Asp340, Gln349	-7.8
Vidofludimus		Rec – Ala251, Arg262, Ile292, Glu323, Pro364; Lig – Arg259, Pro279, Arg319, Gly321, Trp330, Thr332, Ile357, Lys361, Pro279, Met317, Gly335, Phe346, Val350, Tyr360, Gln306, Met317, Thr334, Asp340, Gln349	-7.9
Apremilast		Rec – Ala251, Arg262, Ile292, Glu323, Pro364; Lig – Arg259, Pro279, Arg319, Gly321, Trp330, Thr332, Ile357, Lys361, Pro279, Met317, Gly335, Phe346, Val350, Tyr360, Gln306, Met317, Thr334, Asp340, Gln349	-8.0



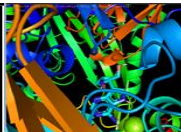
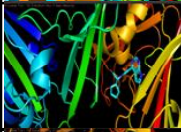
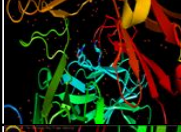
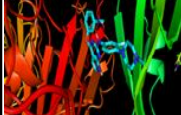
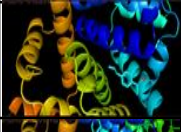
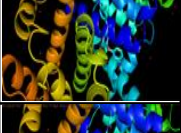
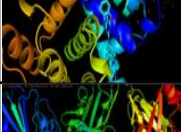
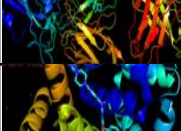
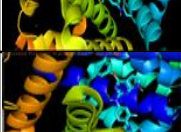

Ibuprofen		Rec – Ala251, Arg262, Ile292, Glu323, Pro364; Lig – Arg259, Pro279, Arg319, Gly321, Trp330, Thr332, Ile357, Lys361, Pro279, Met317, Gly335, Phe346, Val350, Tyr360, Gln306, Met317, Thr334, Asp340, Gln349	-8.1
Ruxolitinib		Rec – Ala251, Arg262, Ile292, Glu323, Pro364; Lig – Arg259, Pro279, Arg319, Gly321, Trp330, Thr332, Ile357, Lys361, Pro279, Met317, Gly335, Phe346, Val350, Tyr360, Gln306, Met317, Thr334, Asp340, Gln349	-8.3
Brensocaticib		Rec – Ala251, Arg262, Ile292, Glu323, Pro364; Lig – Arg259, Pro279, Arg319, Gly321, Trp330, Thr332, Ile357, Lys361, Pro279, Met317, Gly335, Phe346, Val350, Tyr360, Gln306, Met317, Thr334, Asp340, Gln349	-8.4
Carbamic acid		Rec – Ala251, Arg262, Ile292, Glu323, Pro364; Lig – Arg259, Pro279, Arg319, Gly321, Trp330, Thr332, Ile357, Lys361, Pro279, Met317, Gly335, Phe346, Val350, Tyr360, Gln306, Met317, Thr334, Asp340, Gln349	-9.8

Table-4. Molecular docking of selected ligands with RdRp PDB ID: 7JLT protein and their binding energies

Ligand	Protein-ligand interactions	Interacting amino acids	Binding energies (kcal/mol)
Ifenprodil		Rec – Val11, Leu14, Ser15, Gln18, Gln19, Glu23, Trp29, Val33, His36, Asn37; Lig – Val83, Thr84, Met87, Arg80	-5.8
Avitinib		Rec – Val11, Leu14, Ser15, Gln18, Gln19, Glu23, Trp29, Val33, His36, Asn37; Lig – Val83, Thr84, Met87, Arg80	-8.2
ONO-5334		Rec – Val11, Leu14, Ser15, Gln18, Gln19, Glu23, Trp29, Val33, His36, Asn37; Lig – Val83, Thr84, Met87, Arg80	-8.9
Thalidomide		Rec – Val11, Leu14, Ser15, Gln18, Gln19, Glu23, Trp29, Val33, His36, Asn37; Lig – Val83, Thr84, Met87, Arg80	-7.6
Vidofludimus		Rec – Val11, Leu14, Ser15, Gln18, Gln19, Glu23, Trp29, Val33, His36, Asn37; Lig – Val83, Thr84, Met87, Arg80	-8.2
Apremilast		Rec – Val11, Leu14, Ser15, Gln18, Gln19, Glu23, Trp29, Val33, His36, Asn37; Lig – Val83, Thr84, Met87, Arg80	-8.9

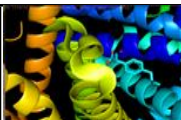



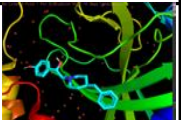
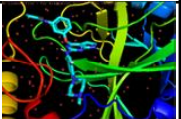
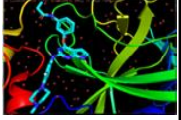
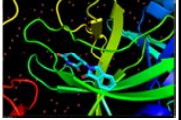
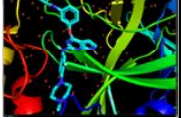
Ibuprofen		Rec – Val11, Leu14, Ser15, Gln18, Gln19, Glu23, Trp29, Val33, His36, Asn37; Lig – Val83, Thr84, Met87, Arg80	-5.6
Ruxolitinib		Rec – Val11, Leu14, Ser15, Gln18, Gln19, Glu23, Trp29, Val33, His36, Asn37; Lig – Val83, Thr84, Met87, Arg80	-7.2
Brensocaticib		Rec – Val11, Leu14, Ser15, Gln18, Gln19, Glu23, Trp29, Val33, His36, Asn37; Lig – Val83, Thr84, Met87, Arg80	-8.4
Carbamic acid		Rec – Val11, Leu14, Ser15, Gln18, Gln19, Glu23, Trp29, Val33, His36, Asn37; Lig – Val83, Thr84, Met87, Arg80	-7.2

Table-5. Molecular docking of selected ligands with Mpro PDB ID: 7ALH protein and their binding energies

Ligand	Protein-ligand interactions	Interacting amino acids	Binding energies (kcal/mol)
Ifenprodil		Rec – Thr24, Thr25, Thr26, Leu27, His41, Cys44, Thr45, Ser46, Met49 Lig – Phe140, Leu141, Asn142, Gly143, Ser144, Cys145, His163, His164, Met165, Glu166, Leu167, Pro168, Arg188, Gln189, Thr190, Gln192	-6.5
Avitinib		Rec – Thr24, Thr25, Thr26, Leu27, His41, Cys44, Thr45, Ser46, Met49 Lig – Phe140, Leu141, Asn142, Gly143, Ser144, Cys145, His163, His164, Met165, Glu166, Leu167, Pro168, Arg188, Gln189, Thr190, Gln192	-7.2
ONO-5334		Rec – Thr24, Thr25, Thr26, Leu27, His41, Cys44, Thr45, Ser46, Met49 Lig – Phe140, Leu141, Asn142, Gly143, Ser144, Cys145, His163, His164, Met165, Glu166, Leu167, Pro168, Arg188, Gln189, Thr190, Gln192	-7.3
Thalidomide		Rec – Thr24, Thr25, Thr26, Leu27, His41, Cys44, Thr45, Ser46, Met49 Lig – Phe140, Leu141, Asn142, Gly143, Ser144, Cys145, His163, His164, Met165, Glu166, Leu167, Pro168, Arg188, Gln189, Thr190, Gln192	-5.6
Vidofludimus		Rec – Thr24, Thr25, Thr26, Leu27, His41, Cys44, Thr45, Ser46, Met49 Lig – Phe140, Leu141, Asn142, Gly143, Ser144, Cys145, His163, His164, Met165, Glu166, Leu167, Pro168, Arg188, Gln189, Thr190, Gln192	-7.2

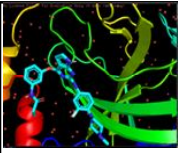
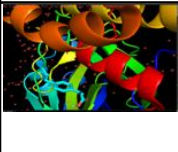


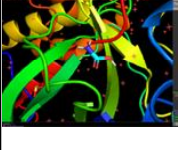

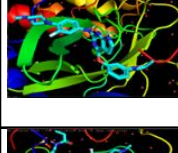

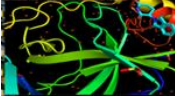
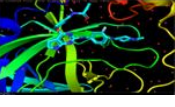
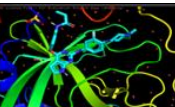
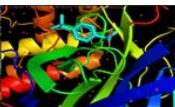
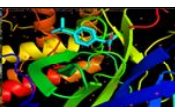
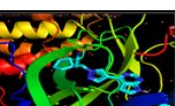
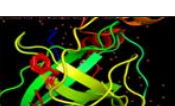
Apremilast		Rec – Thr24, Thr25, Thr26, Leu27, His41, Cys44, Thr45, Ser46, Met49 Lig – Phe140, Leu141, Asn142, Gly143, Ser144, Cys145, His163, His164, Met165, Glu166, Leu167, Pro168, Arg188, Gln189, Thr190, Gln192	-7.0
Ibuprofen		Rec – Thr24, Thr25, Thr26, Leu27, His41, Cys44, Thr45, Ser46, Met49 Lig – Phe140, Leu141, Asn142, Gly143, Ser144, Cys145, His163, His164, Met165, Glu166, Leu167, Pro168, Arg188, Gln189, Thr190, Gln192	-4.8
Ruxolitinib		Rec – Thr24, Thr25, Thr26, Leu27, His41, Cys44, Thr45, Ser46, Met49 Lig – Phe140, Leu141, Asn142, Gly143, Ser144, Cys145, His163, His164, Met165, Glu166, Leu167, Pro168, Arg188, Gln189, Thr190, Gln192	-6.0
Brensocaticib		Rec – Thr24, Thr25, Thr26, Leu27, His41, Cys44, Thr45, Ser46, Met49 Lig – Phe140, Leu141, Asn142, Gly143, Ser144, Cys145, His163, His164, Met165, Glu166, Leu167, Pro168, Arg188, Gln189, Thr190, Gln192	-6.7
Carbamic acid		Rec – Thr24, Thr25, Thr26, Leu27, His41, Cys44, Thr45, Ser46, Met49 Lig – Phe140, Leu141, Asn142, Gly143, Ser144, Cys145, His163, His164, Met165, Glu166, Leu167, Pro168, Arg188, Gln189, Thr190, Gln192	-5.0

Table-6. Molecular docking of selected ligands with PLpro PDB ID: 7AEG protein and their binding energies

Ligand	Protein-ligand interactions	Interacting amino acids	Binding energies (kcal/mol)
Ifenprodil		Rec – Cys22, Gly23, Thr24, Thr25, Thr26, Leu27, His41, Val42, Ile43, Cys44, Thr45, Ser46, Met49, Lys61; Lig – Asn142, Gly143, Cys145, Glu166, Gln189, Val2, Ala3, Asp2	-7.6
Avitinib		Rec – Cys22, Gly23, Thr24, Thr25, Thr26, Leu27, His41, Val42, Ile43, Cys44, Thr45, Ser46, Met49, Lys61; Lig – Asn142, Gly143, Cys145, Glu166, Gln189, Val2, Ala3, Asp2	-8.4
ONO-5334		Rec – Cys22, Gly23, Thr24, Thr25, Thr26, Leu27, His41, Val42, Ile43, Cys44, Thr45, Ser46, Met49, Lys61; Lig – Asn142, Gly143, Cys145, Glu166, Gln189, Val2, Ala3, Asp2	-7.8

Thalidomide		Rec – Cys22, Gly23, Thr24, Thr25, Thr26, Leu27, His41, Val42, Ile43, Cys44, Thr45, Ser46, Met49, Lys61; Lig – Asn142, Gly143, Cys145, Glu166, Gln189, Val2, Ala3, Asp2	-6.3
Vidofludimus		Rec – Cys22, Gly23, Thr24, Thr25, Thr26, Leu27, His41, Val42, Ile43, Cys44, Thr45, Ser46, Met49, Lys61; Lig – Asn142, Gly143, Cys145, Glu166, Gln189, Val2, Ala3, Asp2	-7.7
Apremilast		Rec – Cys22, Gly23, Thr24, Thr25, Thr26, Leu27, His41, Val42, Ile43, Cys44, Thr45, Ser46, Met49, Lys61; Lig – Asn142, Gly143, Cys145, Glu166, Gln189, Val2, Ala3, Asp2	-7.8
Ibuprofen		Rec – Cys22, Gly23, Thr24, Thr25, Thr26, Leu27, His41, Val42, Ile43, Cys44, Thr45, Ser46, Met49, Lys61; Lig – Asn142, Gly143, Cys145, Glu166, Gln189, Val2, Ala3, Asp2	-5.3
Ruxolitinib		Rec – Cys22, Gly23, Thr24, Thr25, Thr26, Leu27, His41, Val42, Ile43, Cys44, Thr45, Ser46, Met49, Lys61; Lig – Asn142, Gly143, Cys145, Glu166, Gln189, Val2, Ala3, Asp2	-7.4
Brensocaticib		Rec – Cys22, Gly23, Thr24, Thr25, Thr26, Leu27, His41, Val42, Ile43, Cys44, Thr45, Ser46, Met49, Lys61; Lig – Asn142, Gly143, Cys145, Glu166, Gln189, Val2, Ala3, Asp2	-7.4
Carbamic acid		Rec – Cys22, Gly23, Thr24, Thr25, Thr26, Leu27, His41, Val42, Ile43, Cys44, Thr45, Ser46, Met49, Lys61; Lig – Asn142, Gly143, Cys145, Glu166, Gln189, Val2, Ala3, Asp2	-3.8

One of the most dangerous pandemic illnesses is COVID-19. For pharma researchers, preventing this viral proliferation in humans is a difficult issue. One of the most crucial therapeutic targets to stop viral replication is the SARS-CoV-2 Mpro protein. In the current investigation, carbamic acid docked against spike protein resulted in the least docking score. Further optimization of these protein-protein interactions and docking could lead to promising drugs against SARS-CoV-2.

#### References :

1. Andrade, B. S., F. D. S. Rangel, N. O. Santos, A.D.S. Freitas, W.R.D.A. Soares, S. Siqueira, and Azevedo (2022). *Front. Pharmacol.*, 11: 590598.
2. Anshumali Mittal *et al* (2004). COVID-19 pandemic: Insights into structure, function and hACE2 receptor recognition by SARS-CoV-2, *PLoS pathog.*
3. Clementel D, and A Del Conte, *et al*

- (2022). *Nucl. Acids Res.*, 50(1): 651-656.
4. Coudert E, S Gehant, E de Castro *et al* (2022). *Bioinformatics.*, 39(1): 2023.
5. Eberhardt J, D Santos-Martins, A.F Tillack and S Forli (2021). *J. Chem. Inf. Model.*, 61(8): 3891-3898.
6. Gasteiger E, C Hoogland, and A Gattiker *et al* (2005). Protein identification and analysis tools on the ExPASy server, John M. Walker (ed.). The Proteomics Protocols Handbook, Humana Press. p. 571-607.
7. Ibezim, A., R. S. Onuku, F. Ntie-Kang, N. J. Nwodo, and M. U. Adikwu, (2021). *Sci. Afr.*, 14: e00970.
8. Kenneth McIntosh (2020). Up-to-date corona virus-disease-2019-COVID-19.
9. Lam, S.D., N. Bordin and C. A. Orengo (2020). *Sci. Rep.*, 10(1): 64-71.
10. Mohan, A., N. Rendine, M.K.S. Mohammed, A. Jeeva, H. F. Ji, and V. R Talluri, (2022). *Mol. Divers.*, 1-17.
11. Štekláč, M., D. Zajaček, L. Bučinský, (2021). *J. Mol. Struct.*, 1245: 130968.
12. Subramanian Boopathi, Adolfo B Poma and Ponmalai Kolandaivel (2021). *J. Biomol. Struct. Dyn.*, 39: 3409-3418.
13. Szklarczyk D, and R Kirsch *et al* (2023). *Nucl. Acids Res.*, 51: 638-646.
14. Tian W, Chen Chang, Lei Xue, Jieliang Zhao and Jie Liang (2018). *Nucl. Acids Res.*, 46(1): 363-367.
15. Trott O and A.J Olson (2010). *J. Comput. Chem.*, 31(2): 455-461.
16. Verma, D., N. Tufchi, K. Pant, and A. Thapliyal, (2020). *Curr trends biotechnol pharm.*, 14(2): 123-133.